A Novel One-Dimensional Electronic State at IrTe₂ Surface

Daiki Ootsuki[1], Hiroyuki Ishii[2], Kazutaka Kudo[2], Minoru Nohara[2], Masaya Takahashi[1], Masafumi Horio[3],
Atsushi Fujimori[3], Teppei Yoshida[4], Masashi Arita[5], Hiroaki Anzai[5], Hirofumi Namatame[5],
Masaki Taniguchi[5,6], Naurang L. Saini[7], and Takashi Mizokawa[8]

¹*Department of Physics, University of Tokyo, Kashiwa, Chiba 277-8561, Japan*
²*Research Institute for Interdisciplinary Science, Okayama University, Okayama 700-8530, Japan*
³*Department of Physics, University of Tokyo, Bunkyo, Tokyo 113-0033, Japan*
⁴*Department of Interdisciplinary Environment, Kyoto University, Sakyo, Kyoto 606-8501, Japan*
⁵*Hiroshima Synchrotron Radiation Center, Hiroshima University, Higashihiroshima, Hiroshima 739-0046, Japan*
⁶*Graduate School of Science, Hiroshima University, Higashihiroshima, Hiroshima 739-8526, Japan*
⁷*Department of Physics, University of Roma "La Sapienza", Piazzale Aldo Moro 2, 00185 Roma, Italy*
⁸*Department of Applied Physics, Waseda University, Shinjuku, Tokyo 169-8555, Japan*

(Received November 23, 2016; accepted October 19, 2017; published online November 8, 2017)

Highly one-dimensional (1D) Fermi sheets are realized at the surface of a layered Ir telluride IrTe₂ which exhibits a stripe-type charge and orbital order below ∼280 K. The 1D Fermi sheets appear in the low temperature range where the stripe order is well established. The 1D Fermi sheets are truncated by the bulk Fermi surfaces, and the spectral weight suppression at the Fermi level deviates from the typical Tomonaga–Luttinger behavior. The 1D band runs along the stripe and is accompanied by several branches which can be derived from the quantization in the perpendicular direction.

When translational motion of electrons is confined in one direction or one dimension (1D), the 1D electrons are expected to form a Tomonaga–Luttinger (TL) liquid in which charge and spin propagate separately.[1–4] The spin–charge separation manifests in single-particle excitation spectrum[5] and has been examined in various systems including carbon nanotube,[6] NbSe₃,[7] PrBa₂Cu₄₋ₓZnₓO₈,[8] Au/Si(111),[9–13] and fabricated quantum wires[14] by means of angle-resolved photoemission spectroscopy (ARPES) and scanning tunneling spectroscopy (STS). The momentum-integrated single-particle spectral function $\rho(\omega)$ exhibits the power-law behavior $|\omega|^\alpha$ for the TL liquids instead of the step function $\theta(\omega)$ for the Fermi liquids. The exponents of the power-law functions are determined by coupling constants K_ρ and K_σ that characterize fluctuations in charge and spin channels.[5] In a realistic system, one can assume $K_\sigma = 1$ due to the spin rotational invariance and obtain the relationship $\alpha = (K_\rho + K_\rho^{-1} - 2)/4$. Most of the photoemission and STS studies on the 1D systems focus on the power-law behavior of the momentum-integrated single-particle spectral function $\rho(\omega)$ although the momentum-resolved single-particle spectral function $\rho_k(\omega)$ contains richer information on the nature of TL liquids. This is partly due to the difficulty of aligning the directions of the 1D objects especially in the case of carbon nanotube. Also in Au/Si(111), NbSe₃, and PrBa₂Cu₄₋ₓZnₓO₈, the interaction between the neighboring 1D objects (Au wire, Nb–Se chain, Cu–O chain) is non-negligible and the Fermi surface is not exactly one-dimensional.

The 1D electron propagating along the x-axis has energy dispersion along the k_x direction in the three-dimensional k-space. Therefore, in the k-space, the Fermi surface of the 1D electron forms two parallel planes that are perpendicular to the k_x direction. Surprisingly, such textbook behavior of the 1D electron has never been observed in the TL liquid candidates including the systems mentioned above. In this context, it is very important to explore a system with ideal 1D Fermi surfaces. If it exists, it is highly interesting to examine the spectral behavior predicted for TL liquids as well as other possible spectral features expected for 1D electrons.

IrTe₂ and related systems have been attracting great interest due to its exotic structural transition around 280 K[15,16] and the superconductivity induced by intercalation or chemical substitution.[17–20] The origin of the structural transition is the Ir 5d/Te 5p charge/orbital order that could be driven by Fermi surface nesting,[21,22] orbitally-induced Peierls effect,[23] Te 5p hole,[24] and/or van Hove singularity.[25] The low-temperature phase of IrTe₂ is expected to have a novel quasi-two-dimensional electronic state due to the Ir 5d/Te 5p charge/orbital order.[26,27] In the previous ARPES study on IrTe₂, in addition to the complicated Fermi sheets of the bulk state with the Ir 5d/Te 5p orbital and charge, straight Fermi sheets are observed in the low temperature phase.[28] The straight Fermi sheets could be consistent with the Ir 5d/Te 5p orbital symmetry breaking and be consistent with the orbitally-induced Peierls mechanism in which 1D Fermi sheets can be formed due to orbital order.[29] However, the straight Fermi sheets were observed only when the IrTe₂ crystals were cleaved at room temperature and then cooled down to the low temperature indicating that the surface preparation and the cooling procedure are important. In order to clarify the origin of the straight Fermi sheets observed in IrTe₂, we have measured photon energy dependence of ARPES which clearly shows its surface origin. The 1D surface band exhibits several surprising features including the branching and the kink. In the following paragraphs, the ARPES results on the 1D surface band of IrTe₂ are presented and the possible origins of the spectral features are discussed.

Single crystal samples of IrTe₂ were prepared using a self-flux method.[30] The single crystals were oriented by ex situ Laue measurements. ARPES measurements were performed at beamline 9A of Hiroshima Synchrotron Radiation Center (HiSOR). The base pressure of the spectrometer of HiSOR BL-9A was in the 10^{-9} Pa range. The crystals were cleaved at 300 K under the ultrahigh vacuum and then cooled to 20 K for the ARPES measurements. The ARPES data were obtained within 12 h after the cleavage. The total energy resolutions were set to 18–29 meV for excitation energies of
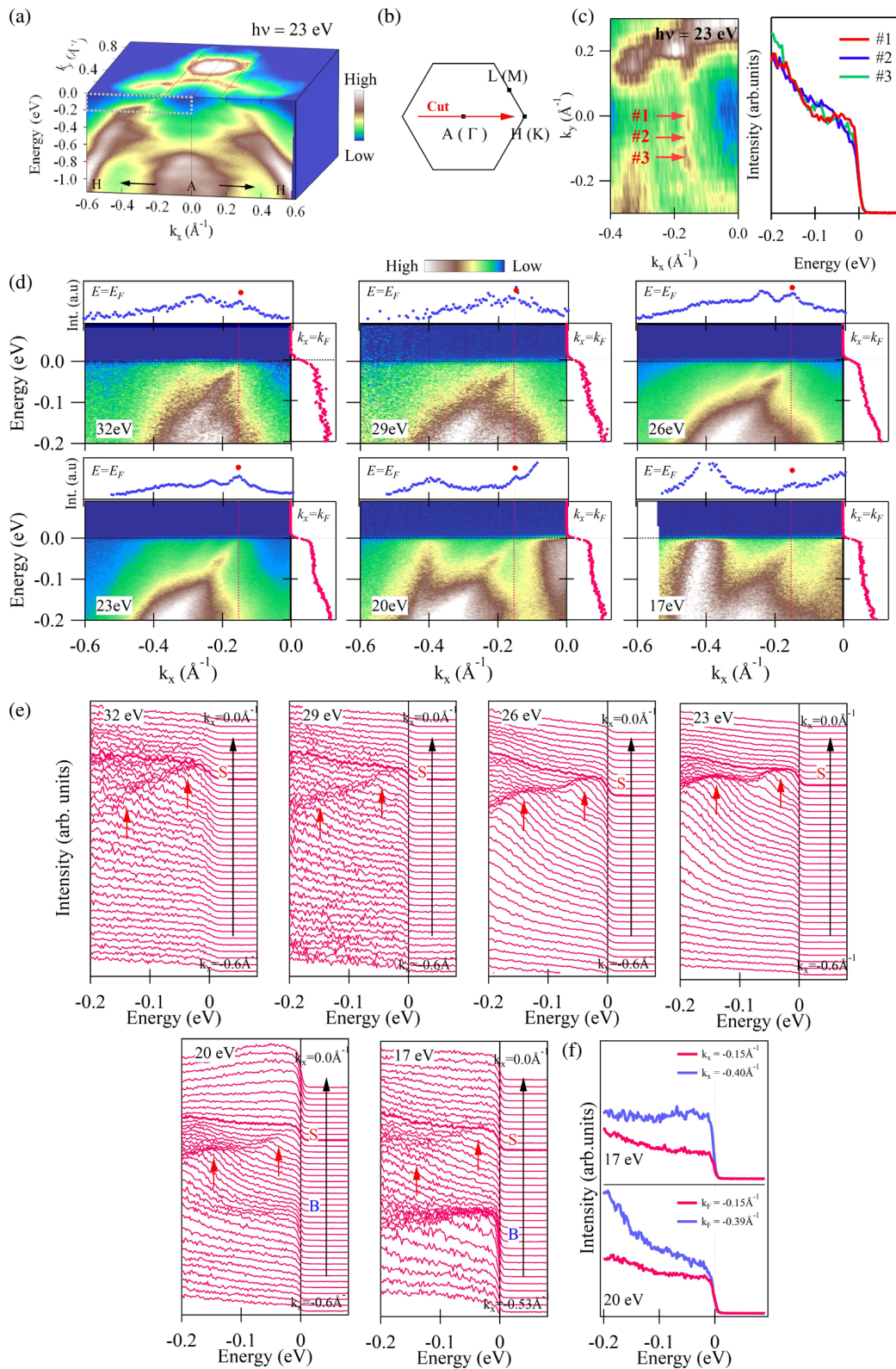
Fig. 1. (Color online) (a) Fermi surface map and band map for IrTe$_2$ at $h\nu = 23$ eV where 1D Fermi surfaces and 1D band dispersions are observed. (b) Brillouin zone of trigonal phase. k_x is along the Γ–K or A–H direction. (c) Fermi surface map and EDCs at several points along the 1D Fermi surface. (d) Band maps with MDCs at E_F and EDCs at k_F of IrTe$_2$ along the k_x direction taken at 20 K and $h\nu = 32, 29, 26, 23, 20$, and 17 eV. The vertical dotted lines roughly indicate k_F at which the surface 1D band crosses E_F. (e) EDCs taken at 20 K and $h\nu = 32, 29, 26, 23, 20$, and 17 eV. The surface and bulk bands are labeled as S and B. (f) EDCs at k_F of the surface and bulk bands.

23–29 eV. Binding energies were calibrated using the Fermi edge of gold reference samples.

Figure 1 shows the ARPES results taken at 20 K for IrTe$_2$. The crystals were cleaved at 300 K and then slowly cooled

down to 20 K for the measurements. The Fermi surface map and the band map at $h\nu = 23$ eV are displayed in Fig. 1(a). The straight Fermi sheets reported by Ootsuki et al.[28] are clearly observed in the Fermi surface map. The 1D band with
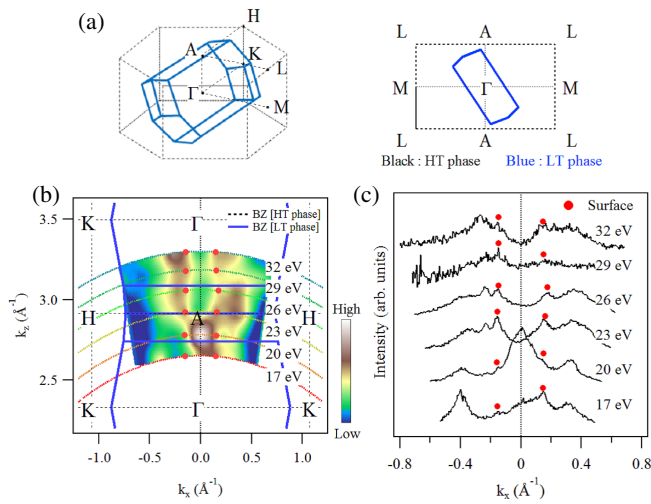
Fig. 2. (Color online) (a) Relation between the trigonal Brillouin zone for high temperature phase (black) and the triclinic Brillouin zone for low temperature phase (blue). (b) Fermi surface map in the k_x–k_z plane. k_z is the electron momentum perpendicular to the cleaved surface. (c) MDCs at E_F taken at $h\nu = 32$, 29, 26, 23, 20, and 17 eV.

Fig. 3. (Color online) (a) Photon energy dependence of EDC obtained at $k_x = -0.18\,\text{Å}^{-1}$. (b) EDC at $h\nu = 23$ eV (dots) taken at the momentum indicated by the vertical dotted line. The EDC is fitted to the five Gaussian curves. The horizontal dashed lines correspond to the peak positions of the Gaussians.

hole character clearly crosses the Fermi level (E_F) in the band map approximately along the k_x direction. Here, k_x is the momentum along the the A–H or Γ–K direction of the bulk 3D Brillouin zone as shown in Fig. 1(b). The 1D band reported in the previous ARPES work[28] is reproduced at $h\nu = 23$ eV including the peculiar spectral weight suppression at point 2 along the 1D Fermi surface as shown in Fig. 1(c). The 1D band dispersions along the k_x direction and including point 1 of Fig. 1(c) are taken at various photon energies and are shown in Fig. 1(d) with momentum distribution curves (MDCs) at E_F and energy distribution curves (EDCs) at the crossing point ($k_x = k_F$). The crossing point k_F of the surface 1D band is indicated by the circle in the MDCs. The 1D band dispersion and k_F hardly depend on the photon energy although the spectral weight changes with the photon energy. Since the momentum perpendicular to the cleaved surface k_z varies with the photon energy, the 1D Fermi sheets are insensitive to k_z indicating its surface origin. The corresponding EDCs taken at various photon energies are shown in Fig. 1(e) where the surface and bulk bands are labeled as S and B. The spectral weight of the 1D surface band is dominant at photon energies higher than 20 eV. The spectral weights near k_F of the 1D surface band and the bulk band are comparable at $h\nu = 20$ and 17 eV and they are compared in Fig. 1(f). In contrast to the spectral weight suppression expected for TL liquids, the surface 1D band exhibits a clear Fermi edge due to the background contribution with the Fermi edge. The background contribution can be estimated at the momentum point where all the valence bands are far from E_F just like Γ point of the cuprate superconductors. Since IrTe$_2$ has various Ir $5d$ and Te $5p$ bands near E_F, it is difficult to estimate the momentum independent background. However, even without the background subtraction, one can see that the EDC peak of the surface band is broad and rounded at E_F whereas it is rather sharp and intense from -0.2 to -0.1 eV and/or from -0.08 to -0.03 eV as indicated by the arrows in Fig. 1(e). In addition, the spectral weight at E_F of the surface band tends to be suppressed compared to that at the bulk band as shown in
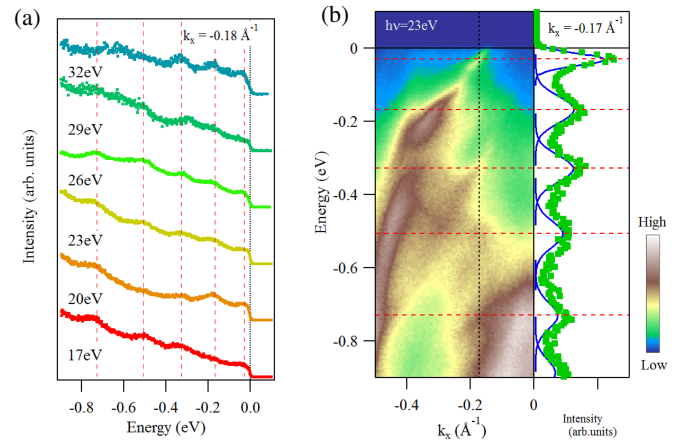
Fig. 1(f). The insufficient suppression of the spectral weight at E_F is not consistent with the TL behavior reported in several 1D or quasi-1D systems.[6–8] The extra spectral weight suppression at point 2 observed at $h\nu = 23$ eV[28] is very difficult to see at other photon energies. Since the 1D surface band and the 1D Fermi sheets are truncated by the bulk band, the deviation from the TL behavior would be related to a kind of spin texture expected in surface states with spin–orbit interaction.

IrTe$_2$ exhibits a complicated charge and orbital order in the low temperature phase. The Brillouin zone is folded with $q = (1/5, 0, -1/5)$ in a complicated manner as illustrated in Fig. 2(a)[18] and the bulk Fermi sheets should be reconstructed accordingly. As shown in the Fermi surface map in the k_x–k_z plane of Fig. 2(b) as well as the MDCs at E_F at various photon energies, the 1D Fermi sheets do not change appreciably with the photon energy or k_z, whereas the other complicated Fermi sheets strongly depend on it. Therefore, the complicated Fermi sheets with the strong k_z dependence can be assigned to the bulk of IrTe$_2$ with Ir/Te orbital and charge order. On the other hand, the straight 1D Fermi sheets should be assigned to the surface state of IrTe$_2$. It is highly interesting how such a 1D electronic state can be realized on the triangular lattice layer of IrTe$_2$.

Since the stripe of the charge orbital order runs along the Ir–Ir or Te–Te direction in the real space (the Γ–M direction in the momentum space) in the bulk IrTe$_2$, it is natural to conclude that the 1D surface band is related to the bulk stripes. This conclusion is also supported from the fact that the 1D band appears only in the low temperature range where the charge/orbital stripes are well established. Since the 2D conducting layer predicted by Toriyama and coworkers[26] is tilted relative to the IrTe$_2$ layer in the bulk charge/orbital ordered state, it should be truncated at the surface. Here, one can speculate that the 1D surface band may correspond to a kind of edge state of the 2D conducting layer of the bulk.

In addition to the main 1D band, several branches are clearly observed well below the Fermi level in Fig. 1(d). Figure 3 shows the photon energy dependence of EDC obtained at $k_x = -0.18\,\text{Å}^{-1}$ in Fig. 1(d). The periodic
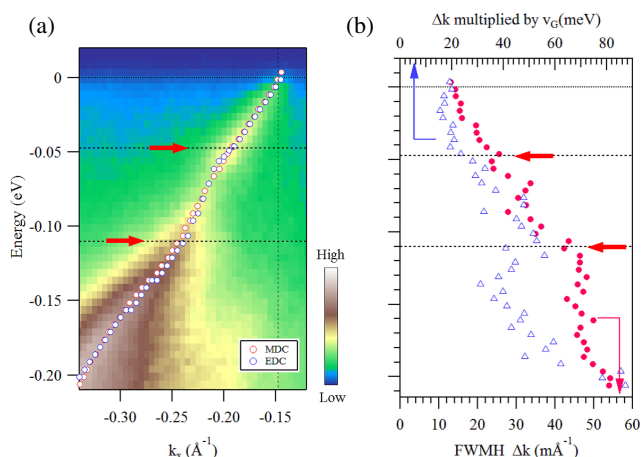
Fig. 4. (Color online) (a) EDCs along the k_x direction taken at $h\nu = 23$ eV. (b) Band map along the k_x direction. (c) Peak positions determined from the EDCs (blue circles) and MDCs (red circles). The positions of the kink at ~50 and ~100 meV are shown by the arrows.

structures of EDC are derived from the several branches of the 1D band as clearly observed in Fig. 3(a). These branches are insensitive to the photon energy, indicating that they are related to the surface 1D band creating the 1D Fermi sheets. In order to further examine the nature of these branches, we have subtracted Shirley type background from the EDC for $h\nu = 23$ eV and fitted the spectrum to the Gaussian functions as shown in Fig. 3(b). These branches suggest that the electrons are confined along the y- and z-directions. The energy separation between the neighboring branches is ~0.15–0.2 eV. Since the velocity of the confined electron V_F is ~1 eV/Å^{-1} as estimated from the slope of the 1D band dispersion from MDCs, the energy separation between the neighboring branches ΔE is ~0.15 eV, the length scale of the confinement would be $\pi V_F/\Delta E \sim 21$ Å.[26,27] Interestingly, this value is comparable to the width of the charge/orbital stripe of the bulk low-temperature phase. This observation indicates that the surface 1D band is affected by the bulk charge/orbital order and is folded into the branches. If the bulk bands are folded with $q = (1/5, 0, -1/5)$, the surface bands are expected to be folded with $q = (1/5, 0, -1/5)$, consistent with the length scale of the confinement or the width of the charge/orbital stripe. Therefore, the branches are expected to form Fermi sheets different from the original one. However, all the branches rapidly lose their spectral weight near E_F and branching of the Fermi sheets is not observed under the present condition.

The straight Fermi sheets are derived from the surface 1D band dispersion along the stripe direction. The band dispersion extracted from EDC agrees with that from MDC as indicated by the open circles in Fig. 4(a). The Fermi velocity v_F of the surface 1D band is estimated from the slope. Interestingly, two kinks are observed in the 1D band dispersion as indicated by the arrows in the band map in Fig. 4(b). In order to estimate the energy scale of the kinks, we estimated the MDC peak width multiplied by the Femi velocity. The energy positions of the kinks are estimated to be 47 and 110 meV, respectively. A Raman spectroscopy study on IrTe$_2$ has reported phonon modes of 21.7, 20.5, 16.9, 16.3, 15.6, and 14.6 meV.[31] None of the phonon

energies agree with the energy scale of the observed kinks. This may indicate that a non-phononic Boson mode interacts with the surface 1D electrons although we cannot exclude the possibility of higher frequency surface phonons. Another interesting point is that the slope of the band dispersion does not change appreciably between the lower and higher energy sides of the kinks. This observation is unusual considering the fact that boson modes responsible for kinks usually causes band renormalization in the lower energy side.[32–35] In the present system, the boson modes should be collective excitations due to electron/spin/lattice interactions responsible for the stripe-type charge and orbital order. The absence of the band renormalization would be reasonable since the kinks are observed in the ordered phase and the collective excitations cannot be the cause of the kinks. Here, we speculate that the kinks observed in the 1D band would be related to Fermionic interactions between the surface and bulk electrons due to the electron correlation[34] or the spin–orbit interaction.

The present result indicates that the surface of IrTe$_2$ and related materials can be a new playground to explore novel 1D electronic states. The 1D electronic state is naturally formed due to the orbital and charge ordering in the bulk. In particular, the strong spin–orbit interaction of the Ir 5d and Te 5p subshells can be exploited for realization of new spintronics or orbitronics devices. The effect of the spin–orbit interaction should be studied in future by means of spin-resolved photoemission spectroscopy.

1) S. Tomonaga, Prog. Theor. Phys. **5**, 544 (1950).
2) J. M. Luttinger, J. Math. Phys. **4**, 1154 (1963).
3) E. H. Lieb and F. Y. Wu, Phys. Rev. Lett. **20**, 1445 (1968).
4) F. D. M. Haldane, Phys. Rev. Lett. **47**, 1840 (1981).
5) J. Voit, J. Electron Spectrosc. Relat. Phenom. **117–118**, 469 (2001).
6) H. Ishii, H. Kataura, H. Shiozawa, H. Yoshioka, H. Otsubo, Y. Takayama, T. Miyahara, S. Suzuki, Y. Achiba, M. Nakatake, T. Narimura, M. Higashiguchi, K. Shimada, H. Namatame, and M. Taniguchi, Nature **426**, 540 (2003).
7) J. Schäfer, M. Sing, R. Claessen, E. Rotenberg, X. J. Zhou, R. E. Thorne, and S. D. Kevan, Phys. Rev. Lett. **91**, 066401 (2003).
8) T. Mizokawa, K. Nakada, C. Kim, Z.-X. Shen, T. Yoshida, A. Fujimori, S. Horii, Y. Yamada, H. Ikuta, and U. Mizutani, Phys. Rev. B **65**, 193101 (2002).
9) J. N. Crain, A. Kirakosian, K. N. Altmann, C. Bromberger, S. C. Erwin, J. L. McChesney, J.-L. Lin, and F. J. Himpsel, Phys. Rev. Lett. **90**, 176805 (2003).
10) J. R. Ahn, P. G. Kang, K. D. Ryang, and H. W. Yeom, Phys. Rev. Lett. **95**, 196402 (2005).
11) K. Nakatsuji, Y. Motomura, R. Niikura, and F. Komori, Phys. Rev. B **84**, 115411 (2011).
12) C. Blumenstein, J. Schäfer, S. Mietke, S. Meyer, A. Dollinger, M. Lochner, X. Y. Cui, L. Patthey, R. Matzdorf, and R. Claessen, Nat. Phys. **7**, 776 (2011).
13) R. Heimbuch, M. Kuzmin, and H. J. W. Zandvliet, Nat. Phys. **8**, 697 (2012).
14) S. Jezouin, M. Albert, F. D. Parmentier, A. Anthore, U. Gennser, A. Cavanna, I. Safi, and F. Pierre, Nat. Commun. **4**, 1802 (2013).

15) S. Jobic, R. Brec, and J. Rouxel, J. Solid State Chem. **96**, 169 (1992).
16) N. Matsumoto, K. Taniguchi, R. Endoh, H. Takano, and S. Nagata, J. Low Temp. Phys. **117**, 1129 (1999).
17) S. Pyon, K. Kudo, and M. Nohara, J. Phys. Soc. Jpn. **81**, 053701 (2012).
18) J. J. Yang, Y. J. Choi, Y. S. Oh, A. Hogan, Y. Horibe, K. Kim, B. I. Min, and S.-W. Cheong, Phys. Rev. Lett. **108**, 116402 (2012).
19) M. Kamitani, S. Bahramy, R. Arita, S. Seki, T. Arima, Y. Tokura, and S. Ishiwata, Phys. Rev. B **87**, 180501(R) (2013).
20) K. Kudo, M. Kobayashi, S. Pyon, and M. Nohara, J. Phys. Soc. Jpn. **82**, 085001 (2013).
21) Y. S. Oh, J. J. Yang, Y. Horibe, and S.-W. Cheong, Phys. Rev. Lett. **110**, 127209 (2013).
22) K. Kim, S. Kim, K.-T. Ko, H. Lee, J.-H. Park, J. J. Yang, S.-W. Cheong, and B. I. Min, Phys. Rev. Lett. **114**, 136401 (2015).
23) D. Ootsuki, Y. Wakisaka, S. Pyon, K. Kudo, M. Nohara, M. Arita, H. Anzai, H. Namatame, M. Taniguchi, N. L. Saini, and T. Mizokawa, Phys. Rev. B **86**, 014519 (2012).
24) A. F. Fang, G. Xu, T. Dong, P. Zheng, and N. L. Wang, Sci. Rep. **3**, 1153 (2013).
25) T. Qian, H. Miao, Z. J. Wang, X. Liu, X. Shi, Y. B. Huang, P. Zhang, N. Xu, P. Richard, M. Shi, M. H. Upton, J. P. Hill, G. Xu, X. Dai, Z. Fang, H. C. Lei, C. Petrovic, A. F. Fang, N. L. Wang, and H. Ding, New J. Phys. **16**, 123038 (2014).
26) T. Toriyama, M. Kobori, Y. Ohta, T. Konishi, S. Pyon, K. Kudo, M. Nohara, K. Sugimoto, T. Kim, and A. Fujiwara, J. Phys. Soc. Jpn. **83**, 033701 (2014).
27) G. L. Pascut, K. Haule, M. J. Gutmann, S. A. Barnett, A. Bombardi, S. Artyukhin, T. Birol, D. Vanderbilt, J. J. Yang, S.-W. Cheong, and V. Kiryukhin, Phys. Rev. Lett. **112**, 086402 (2014).
28) D. Ootsuki, S. Pyon, K. Kudo, M. Nohara, M. Horio, T. Yoshida, A. Fujimori, M. Arita, H. Anzai, H. Namatame, M. Taniguchi, N. L. Saini, and T. Mizokawa, J. Phys. Soc. Jpn. **82**, 093704 (2013).
29) D. I. Khomskii and T. Mizokawa, Phys. Rev. Lett. **94**, 156402 (2005).
30) S. Pyon, K. Kudo, and M. Nohara, Physica C **494**, 80 (2013).
31) N. Lazarević, E. S. Bozin, M. Šćepanović, M. Opačić, H. Lei, C. Petrovic, and Z. V. Popović, Phys. Rev. B **89**, 224301 (2014).
32) A. Lanzara, P. V. Bogdanov, X. J. Zhou, S. A. Kellar, D. L. Feng, E. D. Lu, T. Yoshida, H. Eisaki, A. Fujimori, K. Kishio, J.-I. Shimoyama, T. Noda, S. Uchida, Z. Hussain, and Z.-X. Shen, Nature **412**, 510 (2001).
33) T. Yoshida, K. Tanaka, H. Yagi, A. Ino, H. Eisaki, A. Fujimori, and Z.-X. Shen, Phys. Rev. Lett. **95**, 146404 (2005).
34) K. Byczuk, M. Kollar, K. Held, Y.-F. Yang, I. A. Nekrasov, Th. Pruschke, and D. Vollhardt, Nat. Phys. **3**, 168 (2007).
35) S. R. Park, Y. Cao, Q. Wang, M. Fujita, K. Yamada, S.-K. Mo, D. S. Dessau, and D. Reznik, Phys. Rev. B **88**, 220503(R) (2013).